Electronic Supplementary Material (ESI) for Soft Matter.
This journal is © The Royal Society of Chemistry 2019

Electronic Supporting Information

Magnetowetting dynamics of sessile ferrofluid drops on soft surfaces

Bhaskarjyoti Sarma, Vijay Shahapure, Amaresh Dalal,* and Dipankar N. Basu

[a] *Department of Mechanical Engineering, Indian Institute of Technology Guwahati, Assam - 781039, India.*

*Corresponding Author: *amaresh@iitg.ac.in*

S1. Image processing

a. Image processing for events recorded in camcorder: The image processing of the events of droplet deformation recorded with the Sony camcorder has been carried out in two steps: firstly, the raw images are converted to binary images in ImageJ[1] which helps in defining a sharp interface between the droplet and the surrounding. Subsequently, we carry out manual measurements of the contact angles and contact radius after visually locating the three-phase contact line corresponding to each image. The accuracy of the measurements in contact angle is confirmed by comparing the results from the manual endeavor in ImageJ to that obtained from goniometer for a droplet in equilibrium condition. Also, the converged results obtained from repetitive measurements further confirm the accuracy of measurements.

b. Image processing for events recorded in high-speed camera: For analyzing the images obtained from the high-speed camera we employ a novel methodology by combining the benefits of batch processing mode of ImageJ[1] and an in-house code written in C++. Firstly, the images are processed in batch in ImageJ, wherein we use the following commands in the respective order as given: (i) unsharp mask, (ii) make binary, (iii) fill holes, (iv) outline, (v) make rectangle, and (6) clear outside. The "unsharp mask" command is generally used in image processing for sharpening the interface with the help of a pre-defined Gaussian filter. Next, the "make binary" control divides the image into two intensities thereby prescribing "0 (zero)" value to the interface as well as in the fluid side, whereas "255" to the surrounding. Further, the "fill holes" command is essential for

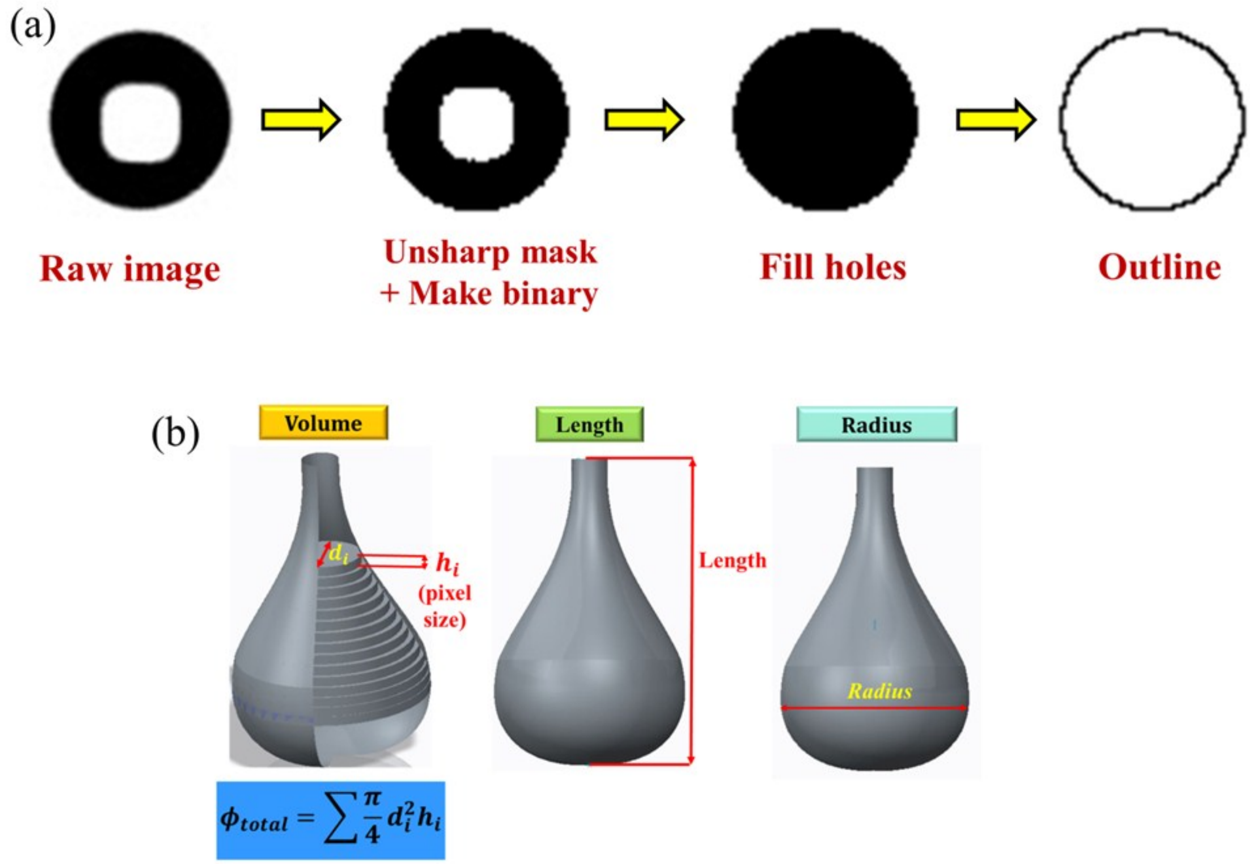

Fig. S1. (a) Sequentially shows different stages of image processing in ImageJ[1] for high-speed events, (b) shows the calculations of different quantitative parameters namely volume, length, and radius.

those events recorded with continuous backlighting as it removes the central white region, which may mislead during edge extraction or any subsequent measurements. The "outline" command as

the name suggests extracts and stores the coordinates and pixels of the edge of the droplet in the form of XYI-data points. The next two steps "make rectangle" and "outline" help us to define a region of interest (ROI) around our object of interest (here the droplet) and to clear the unwanted portion of the image. The novelty of the deigned process flow is that we avoid direct thresholding of the raw image, as mostly done in high-speed stroboscopic events[2], and thereby nullifying the erroneous results that may occur from using a continuous light source[3]. Fig. S1(a) shows the complete process flow as discussed, from converting a raw image to a sharp image.

Next, we feed the coordinates and pixel values extracted from ImageJ to an in-house code, which further analyze the data and provides us the quantitative information of the concerned parameters such as radius (or diameter), area, perimeter, volume, centroid position, area moment of inertia to name a few. For example, the code calculates the volume of a droplet by summing up the volume of each cylindrical slices considered along the vertical axis as shown in Fig. S1(b). The height of these small cylindrical volumes is unit pixel, whereas the radius is found from the two extreme horizontal points considered along same plane. The aforementioned method has been employed effectively for calculating the volume of a droplet from a 2D image in many studies[2,4]. Fig. S1(b) also shows the process employed by the in-house code to measure the droplet radius and length (or height) as per user requirement.

S2. Magnetic Flux density

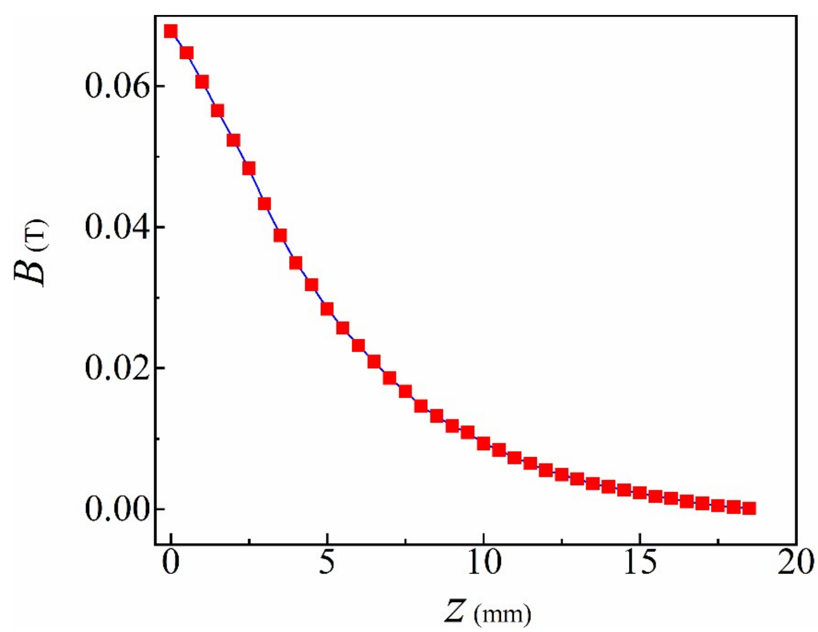

Fig. S2. Magnetic flux density (B) as a function of the vertical gap (H) between the magnet and the PDMS substrate.

Fig. S2 shows that the magnetic flux density, B, decreases as we move away from the magnet surface towards the PDMS substrate. The measurements have been carried out with well-calibrated standard physics laboratory Gaussmeter.

S3. Magnetic Bernoulli equation

The process of continuous elongation by elevating the apex for water-based FF droplets, surrounded by a nonmagnetizable medium, in a non-uniform magnetic field can be explained with the help of augmented magnetic Bernoulli equation[5,6] as written below:

$$p^* + \rho g h + \frac{\rho v^2}{2} - p_m = const. \tag{S1}$$

subjected to the boundary condition,

$$p^* + p_n = p_0 + p_c \tag{S2}$$

where ρ is the density of the ferrofluid, v is the velocity, and n is unit vector normal to the interface.

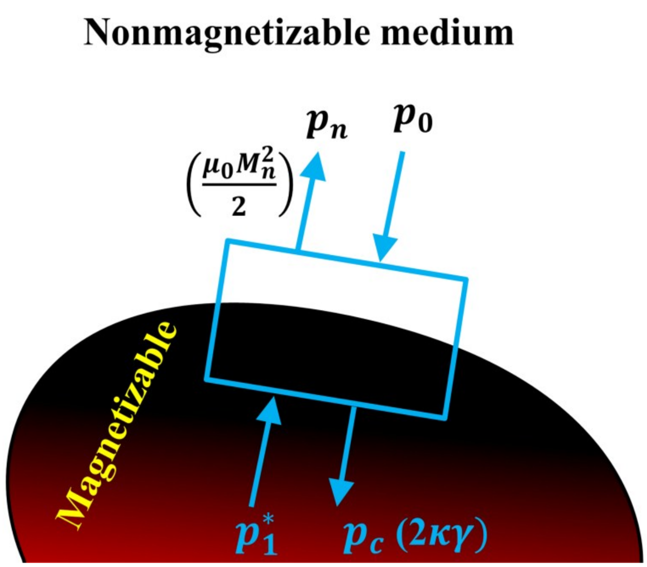

Fig. S3 Schematic representation of the force balance at the interface between the magnetizable liquid medium 1 and nonmagnetizable surrounding 2. The same has been written as FHD boundary condition in Eq. S2.

Eqn. S1 and S2, have been derived considering a sessile FF droplet continuously evolving in a magnetic field of strength, H and following the basic assumption of incompressible, inviscid and isothermal flow. Here, $p_m = \mu_0 \int_0^H M \, dH$ is the fluid magnetic pressure, with M being the magnetization corresponding to and parallel to field H, $p_n = \mu_0 M_n^2/2$, is the magnetic normal pressure with M_n representing the normal component of magnetization, $p_c = 2\kappa\gamma$ is the capillary pressure acting upon a surface having curvature κ, p_0 is pressure of the surrounding nonmagnetic fluid and $p^* = p(\rho,T) + p_m + p_s$ is the modified pressure combining the effect of thermodynamic pressure, $p(\rho,T)$, magnetorestrictive pressure, p_s and the fluid magnetic pressure, p_m. The permeability of vacuum has the value of, $\mu_0 = 4\pi \times 10^{-7}\ N/A^2$. We schematically show the direction of all the pressure components in Fig. S3.

In this study, substituting $v = v_1 = v_2 = 0$ and $p_1 = p_2$, considering a stationary droplet, the magnetic Bernoulli equation, eqn S1, we get Eq. S3 as below,

$$h_2 - h_1 = \frac{\mu_0 H \bar{M}}{\rho g} \tag{S3}$$

where

$$\bar{M} = \frac{1}{H}\int_0^H M \, dH = \frac{1}{H}\int_0^H \chi H \, dH \tag{S4}$$

Here $\bar{M}$ represents average magnetization in the direction of non-uniform field and χ is equal to the initial magnetic susceptibility. Eqn. S3, with a positive right-hand side for water-based FF droplets, clearly explains the continuous elongation and ascent in the sessile condition, which finally triggers splitting of the droplet.

To add further, we can even calculate the magnetic surface force density at the interface by introducing a surface stress tensor, T_m, as below,

$$t_{nn} = nT_m n = p_m + p_n = \mu_0 \int_0^H M\, dH + \frac{\mu_0 M_n^2}{2}. \tag{S5}$$

The surface stress tensor is useful for obtaining the elongation of the FF droplet, where the former is a function of both the magnetic field strength and magnetization of the FF as shown in eqn. S5. Notably, the stress tensor is primarily directed away from the magnetizable medium towards the non-magnetizable medium in case of water-based FFs.

S4. Magnetowetting on a rigid glass surface.

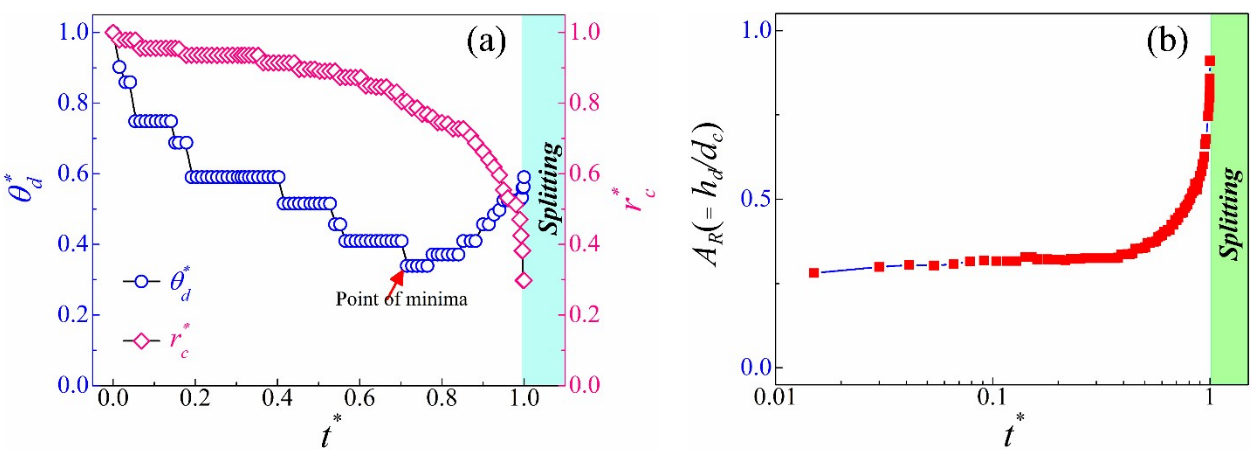

Fig. S4 Magnetowetting dynamics of 4 µL ferrofluid droplet on a clean glass surface. The other experimental parameters are $B_z = 450$ mT and $Bo_m = 131$. Plot (a) shows the temporal variations of the dynamic contact angle, θ_d^*, and contact radius, r_c^*. The non-dimensionalization of the contact angle and radius has been done by the equilibrium values of the concerned parameters. Plot (b) shows the variation of the aspect ratio, $A_R\ (= h_d/d_c)$, with time until the instant of splitting (shaded region). The time scale is non-dimensionalized by the splitting time, t_s.

Figure S4 shows the dynamics of magnetowetting of a 4 µL ferrofluid droplet when exposed to a magnetic field of intensity, $B_z = 450$ mT (corresponding magnetic Bond number, $Bo_m = 131$).

The droplet assumes an initial contact angle, $\theta_{eq} = 40° \pm 1.5°$, on a clean glass slide before the introduction of the magnetic field. The (apparent) dynamic contact angle, θ^*_d (or θ_d) initially decreases and subsequently increases after reaching the point of minima (red arrow), as shown in Fig. S4(a), whereas the contact radius, r^*_c (or r_c) is seen to decrease continuously until the instant of splitting. The anomalous behavior of the trajectory of the contact angle in comparison to the dynamics of magnetowetting on polymeric surfaces, as discussed in the manuscript, can be attributed to the higher wettability of the glass surface. Again, Fig. S4(b) shows the temporal variations of the aspect ratio, A_R $(= h_d/d_c)$, until the instant of splitting, which agrees well with the trend obtained in the case of magnetowetting on polymeric surfaces.

S5. Evaporation of ferrofluid droplets.

We plot the temporal variations in dynamic contact angle, θ_d and contact radius, r_c in Fig. S5(a) and S5(b) for evaporation of a 3 μL FF droplet on substrates with different elasticity (*E* = 1.5, 0.06, and 0.02 MPa) in the absence of magnetic field**.** The temporal scale has been non-dimensionalized with the evaporation time scale, (t_e = 35 min). Further, to help the reader we plot the variations of θ_d and r_c during magnetowetting on same substrate which corresponds to Fig. 2 in the main manuscript ($B = 450\ mT$ and $Bo_m = 131$). It can be discerned clearly that the variations in the concerned quantities are quite sharp during magnetowetting, whereas the contact line dynamics during evaporation has comparatively slower dynamics. The change in the mass of the droplet is also negligible within the time scale of deformation and splitting as shown in Fig. S5(c). This further strengthens our claim that we can neglect the effect of evaporation on the dynamics of magnetowetting.

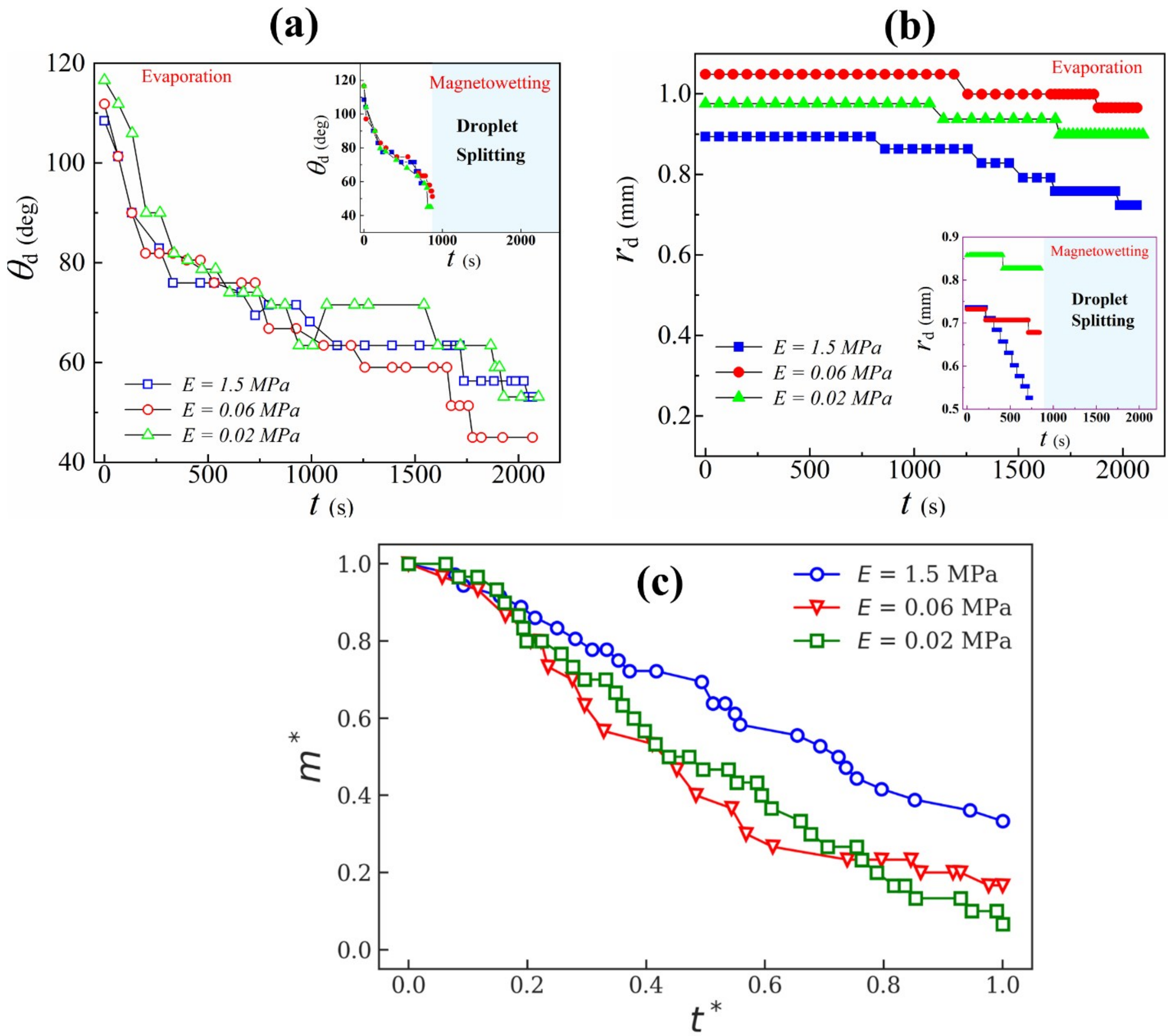

Fig. S5 Temporal variation of the (a) dynamic contact angle, θ_d, and (b) contact radius, r_c during the evaporation of FF droplets ($\phi_0 = 3\ \mu L$) in absence of magnetic field dispensed atop three substrates with different elastic moduli, E = 1.5, 0.06, and 0.02 MPa. The time scale has been non-dimensionalized with the evaporation time scale, (t_e). We show the magnetowetting behavior of the same FF droplets in the inset for B = 450 mT ($Bo_m = 131$). (c) shows the variation of mass of FF droplets during the evaporation events.

6. Supporting Videos

Supporting video S1: The video shows the deformation and splitting of a 3 μL ferrofluid droplet on a PDMS coated glass substrate with elastic moduli, E = 1.5 MPa in the presence of a magnetic field. The magnetic field applied is B_z = 450 mT. The video speed is made faster by 10x.

Supporting video S2: The high-speed video shows the splitting of a 3 μL ferrofluid droplet on a PDMS coated glass substrate with elastic moduli, E = 1.5 MPa in the presence of a magnetic field. The magnetic field applied is B_z = 450 mT. The video speed is made faster by 0.15x.

Supporting video S3: The video shows the deformation and splitting of a 3 μL ferrofluid droplet on a PDMS coated glass substrate with elastic moduli, E = 0.06 MPa in the presence of a magnetic field. The magnetic field applied is B_z = 450 mT. The video speed is made faster by 10x.

Supporting video S4: The high-speed video shows the splitting of a 3 μL ferrofluid droplet on a PDMS coated glass substrate with elastic moduli, E = 0.06 MPa in the presence of a magnetic field. The magnetic field applied is B_z = 450 mT. The video speed is made faster by 0.15x.

Supporting video S5: The video shows the deformation and splitting of a 3 μL ferrofluid droplet on a PDMS coated glass substrate with elastic moduli, E = 0.02 MPa in the presence of a magnetic field. The magnetic field applied is B_z = 450 mT. The video speed is made faster by 10x.

Supporting video S6: The high-speed video shows the splitting of a 3 μL ferrofluid droplet on a PDMS coated glass substrate with elastic moduli, E = 0.02 MPa in the presence of a magnetic field. The magnetic field applied is B_z = 450 mT. The video speed is made faster by 0.15x.

References:

[1] C.A. Schneider, W.S. Rasband, K.W. Eliceiri, Nature Methods, 2012, 9, 671-675.

[2] I. Hutchings, G. Martin, S. Hoath, Journal of Imaging Science and Technology, 2007, 51, 438-444.

[3] J. C. Russ, The image processing handbook, CRC Press, Boca Raton, FL, 2002.

[4] H. Dong, W. W. Carr, J. F. Morris, Physics of Fluids, 2006, 18, 072102.

[5] R. E. Rosensweig, Ferrohydrodynamics, Cambridge University Press, Cambridge; NewYork, 1st edn, 1985.

[6] G. P. Zhu, N. T. Nguyen, R. V. Ramanujan, and X. Y. Huang, Langmuir, 2011, **27**, 14834–14841.